HAL
open science

Tropospheric corrections of SAR interferograms with strong topography. Application to Etna

Christophe Delacourt, Pierre Briole, J. Achache

To cite this version:

Christophe Delacourt, Pierre Briole, J. Achache. Tropospheric corrections of SAR interferograms with strong topography. Application to Etna. Geophysical Research Letters, 1998, 25 (15), pp.2849-2852. 10.1029/98GL02112 . hal-03215371

HAL Id: hal-03215371

https://hal.science/hal-03215371v1

Submitted on 3 May 2021

HAL is a multi-disciplinary open access archive for the deposit and dissemination of scientific research documents, whether they are published or not. The documents may come from teaching and research institutions in France or abroad, or from public or private research centers.

L'archive ouverte pluridisciplinaire **HAL**, est destinée au dépôt et à la diffusion de documents scientifiques de niveau recherche, publiés ou non, émanant des établissements d'enseignement et de recherche français ou étrangers, des laboratoires publics ou privés.

GEOPHYSICAL RESEARCH LETTERS, VOL. 25, NO.15, PAGES 2849-2852, AUGUST 1, 1998

Tropospheric corrections of SAR interferograms with strong topography. Application to Etna

C. Delacourt,[1] P. Briole[1,3] and J.Achache[2]

Abstract. The accuracy of spaceborne geodetic techniques, including SAR interferometry, is limited by the time and spatial variation and altitude dependance of the propagation delay of electomagnetic waves in the lower troposphere, particularly in mountainous areas. In this paper, we use a 1D model developed for tropospheric corrections of GPS and DORIS measurements to correct SAR data. The differential tropospheric delay is computed at each pixel of the interferogram from ground temperature, humidity and pressure using two empirical parameters calibrated from several radiosoundings acquired in various latitude and climate conditions. It is shown that with such a model, given the 3300 meters topography of Etna, tropospheric variations can generate up to 4π phase rotations between the top and the bottom of the volcano. In 16 out of the 20 interferograms processed with images acquired between August 1992 and October 1993, correction of the tropospheric effect reduces the number of fringes associated with the 1991-93 eruption from previous estimates. The remaining deformation is consistant with a deforming source located at a depth of 14±1 km. During the second half of the eruption, the subsidence rate at the top of the volcano is roughly stable at 13±3 mm/month. These values are in good agreement with tiltmeter data collected on Etna during the same period and with the estimated volume of erupted material. No significant deformation can be observed during the last month of eruption. Inflation of the volcano seems to resume immediately after the end of the eruption at a rate of 3 mm/month.

Introduction

Differences in meteorological conditions between acquisitions must be taken into account when processing Synthetic Aperture Radar differential interferograms (InSAR) [*Tarayre and Massonnet*, 1996;*Zebker et al.*, 1997], as the troposphere affects propagation of the electro-magnetic waves. This is particularly critical in mountainous areas due to the existence of complex and variable vertical gradients in the lower troposphere. This effect can be evidenced on previously published interferograms (see North-West part of figure 4a in Massonnet et al, 1995 or figure 3 from Tarayre and Massonnet, 1996) where fringes correlated with the topography can be observed in areas supposed to be free of any ground deformation during the time period covered by the SAR images. Contamination of InSAR data by tropospheric artifacts thus limits the accuracy of measurements of small surface motions especially over large areas. To take this effect into account, it is necessary to correct the interferograms for the tropospheric delay. In this paper, we apply a semi-empirical approach developed for tropospheric corrections of GPS and DORIS measurements [*Baby et al.*, 1988] to the case of SAR interferometry.

Tropospheric excess path

The delay $\Delta\tau$ that affect the propagation of an electromagnetic wave through the troposphere is defined as $\Delta\tau = \tau_\epsilon$-R/c where R is the geometric distance between the satellite and the ground and τ_ϵ the propagation time. Azoulay (1976) showed that the curvature of the ray can be neglected for incidence angles greater than 10° as in the case of ERS-1 (21°). Replacing τ_ϵ by its expression as a function of refractivity N along the ray path s, we obtain :

$$\Delta\tau = \frac{1}{c}\int(1+10^{-6}N(s))ds - \frac{R}{c} = \frac{10^{-6}}{c}\int N(s)ds \quad (1)$$

The *excess path* ΔL may be defined as :

$$\Delta L = c\Delta\tau = \frac{10^{-6}}{cos\theta}\int N(h)dh \quad (2)$$

where h is the vertical elevation and θ the satellite angle of sight which will be considered uniform for all pixels of a SAR image. Using the assumption of an horizontally stratified troposphere, Bean (1966) proposed the following expression for the refractivity N(h) :

$$N(h) = 77.6\frac{P(h)}{T(h)} + 3.73 * 10^5\frac{e(h)}{T^2(h)} \quad (3)$$

where P is the total pressure (in mb), e the water vapor partial pressure, and T the temperature (in K). The excess path can thus be written :

$$\begin{aligned}\Delta L &= \frac{77.6*10^{-6}}{cos\theta}\int\frac{P(h)}{T(h)}dh + \frac{0.373}{cos\theta}\int\frac{e(h)}{T^2(h)}dh \\ &= \frac{1}{cos\theta}(\Delta L_h + \Delta L_\omega) \quad (4)\end{aligned}$$

[1] Institut de Physique du Globe de Paris, France
[2] BRGM, France
[3] CNRS - UMR 7580

Copyright 1998 by the American Geophysical Union.

Paper number 98GL02112.
0094-8534/98/98GL-02112$05.00

The first term of ΔL, which depends on P and T, is known as the hydrostatic component ΔL_h. The second term which depends on T and e, is known as the wet component ΔL_ω. Assuming that the troposphere is an ideal gas in hydrostatic equilibrium, Saastamoinen (1972) showed that ΔL_h could be simply expressed as a function of ground pressure P_g :

$$\Delta L_h = 2.27 * 10^{-3} P_g \quad (5)$$

Wet component of the excess path

Several expressions for ΔL_ω as a function of ground-based meteorological parameters have been proposed in the literature. Assuming that e exponentially decreases and T linearly decreases with elevation, Saastamoinen (1972) proposed the following expression for ΔL_ω :

$$\Delta L_\omega = 2.277 * 10^{-3}(0.005 + \frac{1255}{T_g}) * e_g \quad (6)$$

where T_g and e_g are the values of T and e at ground level. Models for the decrease of water vapor partial pressure as a function of height have been proposed by Smith and Weintraub (1953) and Hopfield (1971). However, field measurements have shown that humidity profiles are in general much more complex [*Baby et al.*, 1988] and impossible to fit with an exponential expression as used by Saastamoinen (1972). Baby et al (1988) made the assumption of a constant humidity rate U=U$_g$ up to a given elevation h_m where it reduces to zero. To better comply with local observations of the troposphere, they introduced in their model two regional parameters adjusted for different climatic conditions (continental, tropical...) and different latitudes to fit the large number of available radio-sounding profiles. Their expression ΔL_ω then reduces to the simple semi-empirical formula :

$$\Delta L_\omega = \nu U_g 10^{\gamma(T_g - 273)} \quad (7)$$

where ν (in mm) ranges from 0.4 for a continental climate near the pole to 0.9 for an oceanic climate at the equator, and $\gamma(inC^{-1})$ ranges from 0.022 for an oceanic climate at tropical latitude to 0.029 for a continental climate at the pole.

Differential tropospheric delay

Expressions (5) and (7) allow us to compute the tropospheric excess path Δ_L of SAR wave from ground-based meteorological data P_g, T_g and U_g :

$$\Delta L = \frac{2.27 * 10^{-3} P_g + \nu U_g 10^{\gamma(T_g - 273)}}{cos\theta} \quad (8)$$

In an interferogram the differential tropospheric delay, at a given pixel is thus :

$$\Delta L_{dif} = \frac{1}{cos\theta}(2.27 * 10^{-3}(P_{g1} - P_{g2}) + \nu U_{g1} 10^{\gamma(T_{g1} - 273)} - \nu U_{g2} 10^{\gamma(T_{g2} - 273)}) \quad (9)$$

Ground values P_{gi}, T_{gi} and U_{gi} depend on the altitude of the corresponding pixel in the image i. They can be expressed as functions of T_0, P_0 and U_0 measured at a reference point of elevation h_0. T is assumed to decrease linearly with h with a gradient k ranging from 0.0055 to 0.0072.

For the pressure, we use the expression defined by Triplet and Roche (1983):

$$P(\Delta h) = P_0(1 - 22.6 * 10^{-6} \Delta h)^{5.26} \quad (10)$$

where $\Delta h = h - h_0$. U is assumed to be constant as discussed in the previous section. Finally, substituting eq(10) into eq(9) and taking $U_g = U_0$ leads to the following expression for ΔL_{dif} :

$$\Delta L_{dif} = \frac{2.27 * 10^{-3}(P_{01} - P_{02})}{cos\theta}(1 - 22.6 * 10^{-6} \Delta h)^{5\ 26} + \frac{\nu}{cos\theta}(U_{01} 10^{\gamma(T_{01} - 273 - k\Delta h)} - U_{02} 10^{\gamma(T_{02} - 273 - k\Delta h)}) \quad (11)$$

Tropospheric correction of interferograms of Etna

To compute the differential tropospheric delay on Mt Etna, we used daily ground-based data measured at the meteorological station of Serra La Nave (SLN) in the western part of the volcano at 1750 m and the radio sounding profiles carried out, almost at the time of the SAR image acquisition, at the Trapani meteorological station located 200 km West of Etna (Figure 1). The profiles show a systematic thermal inversion between ground level and 500 m height as expected for night-time profiles. Above 500 m, the temperature decreases roughly linearly with a vertical gradient of -0.0068 (value averaged over all available soundings). To compute the excess path from those data, we used eq(11) and values of γ and ν extracted from Baby et al (1988) to fit with the Etna area. Tropospheric corrections were computed on 20 interferograms created by

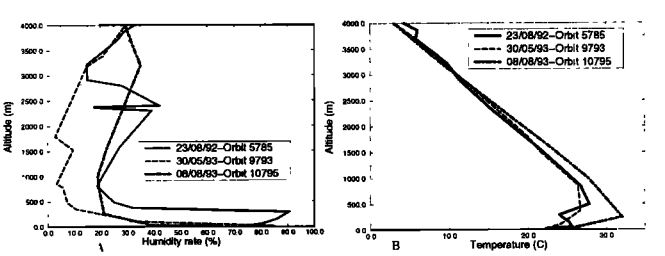

Figure 1. Radio-sounding profiles associated with the interferograms shown on figure 2. (A) Humidity profiles. Complexity of the profiles is clearly visible in these data. (B) Temperature profiles.

CNES with the images acquired between August 1992 and October 1993 and previously analyzed by Massonnet et al. (1995). The tropospheric correction reaches 2 fringes for some interferograms. Figure 2 shows an example of two interferograms before and after tropospheric correction (corresponding radiosounding data are plotted on Figure 1). Both interferograms start on 23/08/92 and span respectively 280 and 350 days. The difference between both is located after the end of the eruption period in which no significant deformation is observed on Etna by classical means (Bonnaccorso, 1996). Similar amount of deformation is thus expected on both interferograms. Figure 2a and 2b show a difference of 2 fringes (5.6 cm) prior to tropospheric correction, and this discrepancy dissapears when tropospheric correction is applied (Figure 2c and 2d). This example illustrates how much our correction can improve the accuracy of interferograms of Etna. In average on all interferograms that we examinated, we estimate a final accuracy after tropospheric correction is about ± 1 fringe (2.8 cm). The residuals should be due mainly to the 3D heterogeneities of the real troposphere and the inospheric noise.

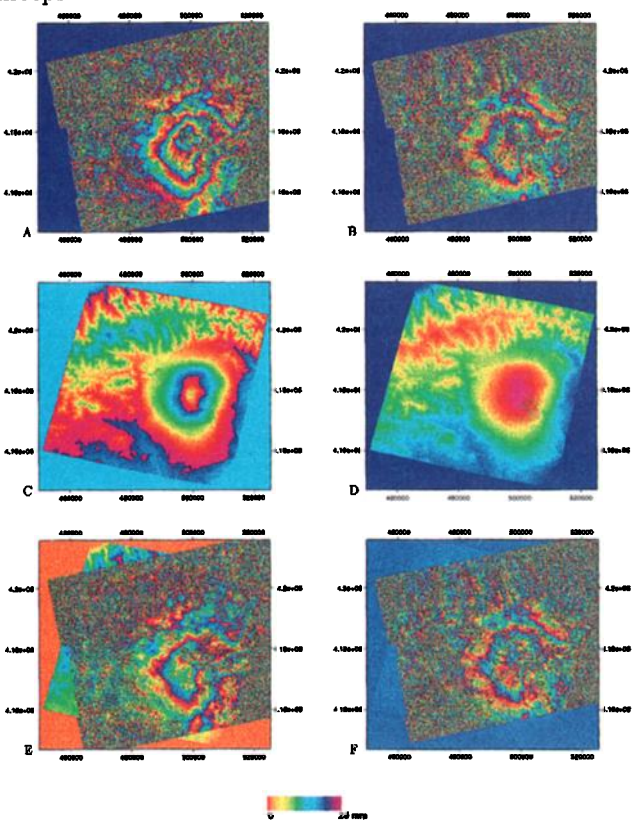

Figure 2. Example of tropospheric effect on differential SAR interferograms of ETNA. (A) 5785-9793 differential interferogram (B) 5785-10795 differentiel interferogram. (C) Tropospheric correction for couple 5785-9793 deduced from meterological conditions plotted on figure 1. (D) Tropospheric correction for couple 5785-10795 deduced from meterological conditions plotted on figure 1. (E) 5785-9793 differential interferogram after tropospheric correction. (F) 5785-10795 differential interferogram after tropospheric correction.

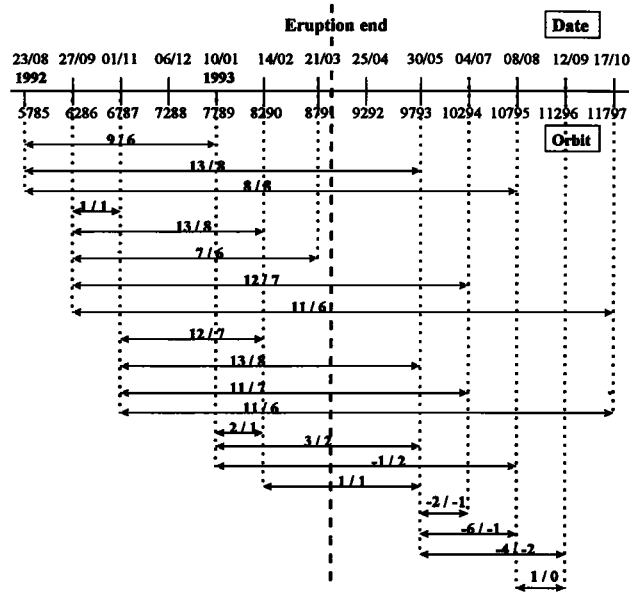

Figure 3. Subsidence of the summit of Etna (in cm) observed between 23/08/92 and 17/10/93. First bold number corresponds to maximum displacment observed without tropospheric correction, second one after tropospheric correction. Uncertainty on the results is 3 cm.

Discussion

In a previous study, Massonnet et al. (1995) interpreted the fringes observed on 1992-93 interferograms of Etna (without tropospheric correction) as the sum of a regional volcano-wide ground subsidence due to the 1991-93 eruption and local deformation associated with recent emplacements of the 1986-87 and 1989 lava flow further modeled by Briole et al. (1996). Here, we use the 6 ascending pairs published in their work plus 14 additional ascending pairs which presented enough coherence (Fig 3). Low value of coherence of some interferograms in relatively large areas prevents us to estimate the deformation by comparing the observed interferogram with a synthetic interferogram of deformation calculated using a Mogi model (1958). The fringes can be satisfactorly accounted for by the deformation resulting from a deflating source at 14±1 km depth. This depth could be further reduced by 1 km taking into account the effect of the volcano topography [*Cayol*, 1996]. The maximum deformation recorded on each interferogram after tropospheric correction is plotted on figure 3. Assuming a steady state rate of subsidence of the volcano until one month prior to the end of the eruption, we obtain a value of 13±3 mm/month for the subsidence rate (Fig 3, against 20 mm/month without any tropospheric correction, Massonnet et al, 1995). The steady state assumption is consistant with the lava flow volume and the relatively steady state tilting rate measured a 4 locations during the 16 months of eruption [*Bonaccorso*, 1996]. No significant deformation is observed during the last month of the eruption. Finally

the data indicate a slow inflation of the volcano after the eruption's end at a rate of 3 mm/month. These rates are in good agreements with the observations of Bonaccorso (1996). At 3 stations, MDZ, DAM and SPC, the average measured tilt over the last 7 months of eruption is 7 μradians, and the corresponding tilt deduced from our model is 5.5 μradians. Only tilt data collected at MSC station (21 μradians) is larger than predicted by interferometry. This difference could be explained by a local deformation which is not taken into account in the Mogi model. MSC tilt data may also be affected by an uncorrected long term drift. Estimation of the effusive rate deduced from interferometric data using the Mogi model is $12.5 * 10^6 m^3$/month which is in good agreement with the value of $14 * 10^6 m^3$/month deduced from Stevens et al (1997). However, given the uncertainty of the interferograms (± 1 fringe), data of figure 3 are not unconsistant with a more complex scenario in which a slow steady-state deflation phase, say around 5 mm/month, is followed by the rapid collapse of the volcano nearly one month prior to the end of the eruption. Such a discontinuous and non elastic behaviour would better fit with the tiltmeter data reccorded at station MSC (Bonaccorso, 1996).

Conclusion

This study shows that tropospheric corrections on ERS interferograms of Etna can account for 6±3 cm, including the error due to lateral and temporal heterogeneities as well as ionospheric artefact not introduced in this study. Monitoring volcanic deformation with SAR interferometry is thus limited at the regional scale and meteorological data are required at one or several location of the investigated area to reach a cm accuracy. Simultaneous GPS measurements would be a very efficient method to improve the meteorological corrections [*Bock and Williams*, 1997]. Static tropospheric correction is essential on sites where the topography may be less strong than on Etna but where the surface deformation accuracy required is close to the limits of interferometry. The new analysis of the 1992-1993 interferograms presented in this paper which accounts for this tropospheric correction leads to a more accurately knowledge of the deformation of Etna during the 1991-93 eruption. Assuming a steady state rate of subsidence of the volcano, the subsidence rate is 13±3 mm/month till one month prior eruption stops. No deformation occurs during the last month of eruption. Slow inflation of the volcano starts 3 mm/month after eruption stops. These results are in good agreement with both tiltmeter data collected at several stations during the eruption and with the volume of the material erupted. Further joint modeling of data (tilt, GPS, SAR) would probably lead to an improved determination of the depth and geometry of the deflating source.

Acknowledgments. We thank Prof. Rodono from the Osservatorio Astrofisico di Serra la Nave for providing the ground meteorological data. We are grateful to A. Bonnacorso, B. Fruneau, F. Sigmundsson and an anonymous reviewer for their constructive comments. This work was supported by the EC program ENV4-CT96-0294. IPGP contribution 1544.

References

Azoulay, A., Etude de l'influence de la troposphère sur la mesure de distance terre-satellite , *Note technique C.N.E.T , NT/EST/APH/34,* 1976.

Baby, H., Gole, P., and Lavergnat, J., A., Model for tropospheric excess path length of radio waves from surface meteorological measurements, Radio Sci., *22,* 1023-1038, 1988.

Bean, B. R., Dutton E. J., Radio meteorology, *Monography, Natl. Bur. of Stand., Gaithersburg,* 1966.

Bock, Y., and Williams, S., Integrated satellite interferometry in southern california , *EOS, 78,* 293-300, 1997.

Bonaccorso, A., Dynamic inversion of ground deformation data for modelling volcanic sources (Etna 1991-93), Geophys. Res. Lett., *23,* 451-454, 1996.

Briole, P., Massonnet, D., and Delacourt, C., Post-eruptive deformation associated with the 1986-87 and 1989 lava flows of Etna, Geophys. Res. Lett., *24,* 37-40, 1996.

Cayol, V., Analyse élastostatique tridimensionnelle du champ de déformations des édifices volcaniques par éléments frontières mixtes, Thesis Paris VII, 1996.

Hopfield, H. S., Tropospheric effect on electromagnetically measured range: prediction from surface weather data, Radio Sci., *6,* 230-241, 1971.

Massonnet, D., Briole, P., and Arnaud, A., Deflation of Mount Etna monitored by spaceborne radar interferometry, , *375,* 567-570, 1995.

Mogi, K., Relations between the eruptions of various volcanoes and the deformation of the ground surface around them, *Bull. Earthquake Res. Inst., 36,* 99-134, 1958.

Saastamoinen, J., Contribution to the theory of atmospheric refraction, *Bull. Géodés., 105,* 279-298, 1972.

Smith, E. K., and Weintraub, S., The constants in the equation of atmospheric refractive index at radio frequencies, *Proceedings of the IRE,* 1035-1037, 1953.

Stevens, N. F., Murray, J. B., and Wadge, G., The volume and shape of the 1991-1993 lava flow field at Mount Etna, Sicily, *Bull. Volcanol., in press,* 1997.

Tarayre, H., and Massonnet, D., Atmospheric propagation heterogeneities revealed by ERS-1 interferometry, Geophys. Res. Lett., *23,* 989-992, 1996.

Triplet, J. P., and Roche, C., *Météorologie générale,* 300 pp., Météofrance, 1983.

Zebker, H. A., Rosen, P. A., and Hensley, S., Atmospheric effects in interferometric synthetic aperture radar surface deformation and topographic maps, J. Geophys. Res.,*102,* 7547-7563, 1997.

C. Delacourt, P. Briole, Institut de Physique du Globe de Paris, 4 Place Jussieu, 75252 Paris Cedex 05, France

J.Achache, BRGM, Research Division, Ave. de Concyr, B.P.6009, 45060 Orléans Cédex 2, France

(received January 30, 1998; revised March 17, 1998; accepted June 2, 1998.)